

Improvement of Renormalization-Scale Uncertainties Within Empirical Determinations of the b -Quark Mass

M.R. Ahmady,^a V. Elias,^b A. Squires,^{b,c} T.G. Steele,^d
Ailin Zhang^{d,e}

^a*Department of Physics, Mount Allison University, Sackville, New Brunswick,
E4L 1E6, Canada*

^b*Department of Applied Mathematics, The University of Western Ontario,
London, Ontario N6A 5B7, Canada*

^c*Newman Laboratory of Nuclear Physics, Cornell University, Ithaca, NY 14853,
USA*

^d*Department of Physics and Engineering Physics, University of Saskatchewan,
Saskatoon, SK, S7N 5E2, Canada*

^e*Department of Physics, Suzhou University, Suzhou, Jiangsu, 215006, China*

Abstract

Accurate determinations of the $\overline{\text{MS}}$ b -quark mass $m_b(m_b)$ from $\sigma(e^+e^- \rightarrow \text{hadrons})$ experimental data currently contain three comparable sources of uncertainty; the experimental uncertainty from moments of this cross-section, the uncertainty associated with $\alpha_s(M_z)$, and the theoretical uncertainty associated with the renormalization scale. Through resummation of all logarithmic terms explicitly determined in the perturbative series by the renormalization-group (RG) equation, it is shown that the renormalization-scale dependence is virtually eliminated as a source of theoretical uncertainty in $m_b(m_b)$. Furthermore, such resummation techniques improve the agreement between the values of the $\overline{\text{MS}}$ b -quark mass extracted from the various moments of $R(s) = \sigma(e^+e^- \rightarrow \text{hadrons})/\sigma_{pt}$ [$\sigma_{pt} = 4\pi\alpha^2/(3s)$], obviating the need to choose an optimum moment for determining $m_b(m_b)$. Resummation techniques are also shown to reduce renormalization-scale dependence in the relation between b -quark $\overline{\text{MS}}$ and pole mass and in the relation between the pole and $1S$ mass.

Key words: bottom quark mass, renormalization group, perturbative QCD
PACS: 12.38.-t; 12.38.Cy; 14.65.Fy

1 Introduction

Comparison of theoretical and experimental moments M_N , defined by

$$M_N = \int \frac{ds}{s^{N+1}} R(s) \quad , \quad N = 1, 2, 3 \dots \quad (1)$$

$$R(s) = \frac{\sigma(e^+e^- \rightarrow \text{hadrons})}{\sigma_{pt}} \quad , \quad \sigma_{pt} = \frac{4\pi\alpha^2}{3s} \quad , \quad (2)$$

provides a method for determining the $\overline{\text{MS}}$ quark masses [1]. This method, combined with recent BES data [2] (particularly in the charm threshold region) and $\mathcal{O}(\alpha_s^2)$ (mass-dependent) perturbative expressions for the moments M_N and for $R(s)$ in the continuum region [3], has resulted in precision determinations of the $\overline{\text{MS}}$ charm and bottom quark masses [4].

The $\overline{\text{MS}}$ b -quark mass determined in [4] contains three major sources of uncertainty;

- (1) experimental values of resonance and threshold contributions within $R(s)$,
- (2) uncertainty in $\alpha_s(M_Z)$, which enters both the perturbative series for M_N and the QCD continuum contribution to experimental moments,
- (3) and theoretical uncertainty associated with renormalization scale dependence within the M_N perturbative series.

In the b -mass estimates of Ref. [4], these three sources of uncertainty play different roles as N varies, but are generally comparable in magnitude. Thus as experimental information becomes more precise, the theoretical uncertainty devolving from renormalization-scale dependence will become increasingly significant.

Techniques for substantially decreasing renormalization scale dependence have been developed and applied to a number of $\overline{\text{MS}}$ perturbative processes including semileptonic b decays, light-quark contributions to $R(s)$, and Higgs decays [5]. These techniques use the appropriate renormalization-group (RG) equation for each process to determine and resum all logarithmic contributions in the perturbation series that are explicitly determined by the RG equation. In this paper we extend and apply such techniques to the perturbative series for the b -quark contributions to M_N , effectively eliminating their renormalization-scale dependence as a source of theoretical uncertainty.

In Section 2, we develop an analysis of the $\mathcal{O}(25 \text{ MeV})$ residual renormalization-scale dependence characterizing the extraction of the $\overline{\text{MS}}$ b -quark mass from the first four moments of $R(s)$. In Section 3, we demonstrate how this scale dependence is essentially eliminated upon incorporating the closed-form summation of leading and successively-subleading logarithms within the perturba-

tive series for $N = \{1, 2, 3, 4\}$ moments of b -quark contributions to $R(s)$. This procedure is also shown to reduce theoretical uncertainties associated with the choice of N , as well as leading to a modest (14 MeV) elevation in the central value for $m_b(m_b)$.

Renormalization-scale dependence is also shown to exist as a source of uncertainty in the known perturbative expressions relating the b -quark $\overline{\text{MS}}$ mass to its corresponding pole mass [6] and $1S$ mass [7,8]. In Section 4 we explore the scale dependence inherent in the perturbative series relating $\overline{\text{MS}}$ and pole b -quark masses. In Section 5, we demonstrate how this uncertainty is resolved by a renormalization-group resummation of this series similar to that of Section 3. Finally, in Section 6 we discuss the reduction of scale uncertainty via comparable renormalization-group resummation of the relationship between the $1S$ and pole b -quark masses.

2 Residual Scale Uncertainty of the $\overline{\text{MS}}$ b -quark Mass

Following Ref. [1], Kühn and Steinhauser [4] express the running b -quark $\overline{\text{MS}}$ mass $m_b(\mu)$ from moments of the b -quark contribution to the experimentally determined electron-positron-annihilation ratio

$$M_N^{exp} \equiv \int \frac{ds}{s^{N+1}} R_b(s) \quad (3)$$

and its ($\overline{\text{MS}}$) field-theoretical analogue

$$M_N^{th} = \left(\frac{1}{4m_b^2(\mu)} \right)^N S_N(\mu) , \quad (4)$$

with the perturbative series S_N related to $\Pi_b(q^2)$, the b -quark contribution to the vector-current correlation function, via

$$\Pi_b(q^2) = \frac{1}{12\pi^2} \sum_N \left(\frac{q^2}{4m_b^2(\mu)} \right)^N S_N(\mu) . \quad (5)$$

If one equates the experimental and theoretical moments, one finds that

$$m_b(\mu) = \frac{1}{2} \left(\frac{S_N(\mu)}{M_N^{exp}} \right)^{\frac{1}{2N}} . \quad (6)$$

| | $N = 1$ | $N = 2$ | $N = 3$ | $N = 4$ |
|-----------------|---------|---------|----------|---------|
| $T_{0,0}^{(N)}$ | 0.2667 | 0.1143 | 0.06772 | 0.04618 |
| $T_{1,0}^{(N)}$ | 0.6387 | 0.2774 | 0.1298 | 0.05775 |
| $T_{1,1}^{(N)}$ | -0.5333 | -0.4571 | -0.4062 | -0.3694 |
| $T_{2,0}^{(N)}$ | 0.7898 | 0.8080 | 0.5169 | 0.3051 |
| $T_{2,1}^{(N)}$ | -0.8606 | -1.2610 | -1.11454 | -0.8682 |
| $T_{2,2}^{(N)}$ | 0.0222 | 0.4762 | 0.8296 | 1.1236 |

Table 1

Five-flavour ($n_f = 5$) $\overline{\text{MS}}$ series coefficients for S_N .

The series S_N is a perturbative series in the QCD couplant $x(\mu) = \alpha_s(\mu)/\pi$, where μ is the renormalization scale characterizing M_N^{th} :

$$S_N(\mu) = \sum_{j=0}^{\infty} \sum_{k=0}^j T_{j,k}^{(N)} x^j(\mu) \log^k \left(\frac{\mu^2}{m_b^2(\mu)} \right), \quad (7)$$

where the $j = \{0, 1, 2\}$ [*i.e.*, up to three-loop] $\overline{\text{MS}}$ coefficients of this series [3] (summarized in Table 6 of Ref.[4]), are tabulated in Table 1.¹ Since S_N has logarithmic dependence on $m_b(\mu)$, Eq. (6) represents an implicit equation that must be solved numerically to determine $m_b(\mu)$.

The theoretical expression (4) for the moments M_N is formally independent of the renormalization scale μ , as expected for this physically-observable quantity.² Thus the requirement $0 = dM_N^{th}/d\mu^2$ leads to the following renormalization-group equation for the series $S_N(\mu)$:

$$0 = \left[(1 - 2\gamma(x)) \frac{\partial}{\partial L} + \beta(x) \frac{\partial}{\partial x} - 2N\gamma(x) \right] S_N[x, L] \quad (8)$$

where $n_f = 5$ and³

$$L(\mu) \equiv \log \left(\mu^2/m_b^2(\mu) \right), \quad (9)$$

$$S_N(\mu) = S_N[x(\mu), L(\mu)] = \sum_{j=0}^{\infty} \sum_{k=0}^j T_{j,k}^{(N)} x^j L^k, \quad (10)$$

¹ Our coefficients $T_{j,k}^{(N)}$ are related to those of Ref. [4]'s Table 6 by $T_{j,k}^{(N)} = (-1)^k c_n^{(j,k)}/4$. Division by 4 is a consequence of $Q_b^2 = Q_c^2/4$. The alternation in sign follows from the argument of our logarithm in Eq. (7) being the inverse of that for the logarithm in the series \tilde{C}_N of Ref. [4].

² The experimental values for M_N are tabulated in Table 7 of Ref. [4]

³ See Refs. [10,11] and Refs. [12,13] for the coefficients in $\beta(x)$ and $\gamma(x)$, respectively.

$$\gamma(x) = \frac{\mu^2}{m_b(\mu)} \frac{dm_b(\mu)}{d\mu^2} = -x \left[1 + \sum_{n=1}^{\infty} \gamma_n x^n \right], \quad (11)$$

$$\gamma_1 = \frac{253}{72}, \quad \gamma_2 = 7.41986, \quad (12)$$

$$\beta(x) = \mu^2 \frac{dx(\mu)}{d\mu^2} = -x^2 \sum_{n=0}^{\infty} \beta_n x^n, \quad (13)$$

$$\beta_0 = \frac{23}{12}, \quad \beta_1 = \frac{29}{12}, \quad \beta_2 = 9769/3456. \quad (14)$$

For example, one finds from Eq. (8) that the coefficients $T_{1,1}^{(N)}$, $T_{2,2}^{(N)}$ and $T_{2,1}^{(N)}$ satisfy the relations

$$T_{1,1}^{(N)} = -2NT_{0,0}^{(N)}, \quad (15)$$

$$T_{2,2}^{(N)} = N(2N - \beta_0)T_{0,0}^{(N)}, \quad (16)$$

$$T_{2,1}^{(N)} = (\beta_0 - 2N)T_{1,0}^{(N)} - 2N(\gamma_1 - 2)T_{0,0}^{(N)}, \quad (17)$$

consistent (modulo round-off errors) with the entries in Table 1.

We are interested in exploring both the residual renormalization scale dependence and the N -dependence of the \overline{MS} benchmark mass m_b (m_b) extracted in Ref. [4], since each such dependence is a source of theoretical uncertainty. As in Ref. [4], the series (7) for $S_N(\mu)$ is truncated after its (known) $j = 2$ terms. Such truncation necessarily becomes a source of residual μ dependence. Since we are focusing *only* on theoretical uncertainties arising from such scale dependence, we assume that $x(\mu)$ four-loop evolves from its Ref. [4] benchmark value $x(M_z) = 0.11800/\pi$ to $x(10 \text{ GeV}) = 0.056732$, and disregard theoretical uncertainty associated with $x(M_z)$ [and hence $x(10 \text{ GeV})$]. The preferred renormalization scale in Ref. [4] for extracting m_b (m_b) is 10 GeV, and as in Ref. [4], the scale dependence we consider is over the range $5 \text{ GeV} \leq \mu \leq 15 \text{ GeV}$. The extraction of m_b (m_b) occurs first by numerical solution of Eq. (4) to obtain $m_b(\mu)$, and then by evolving $m_b(\mu)$ downward via Eq. (11) to the point where $\mu = m_b(\mu) \equiv m_b(m_b)$.

In Table 2, we list the above-described extractions of $m_b(\mu)$ for $\mu = 5, 10$ and 15 GeV , as obtained from each of the $N = \{1, 2, 3, 4\}$ moments using values for M_N^{exp} from Table 7 of Ref. [4].⁴

The column $\overline{m_b}(\mu)$ of Table 2 is just the average of $m_b(\mu)$ taken over the first four moments. The rms spread of values over the first four moments is

$$\sigma_N = \frac{1}{2} \left[\sum_{N=1}^4 \left(m_b^{(N)}(\mu) - \overline{m_b^{(N)}}(\mu) \right)^2 \right]^{1/2}. \quad (18)$$

⁴ Table 2 numbers for $\mu = 10 \text{ GeV}$ are in agreement with those of Ref. [4]’s Table 8.

| μ | $N = 1$ | $N = 2$ | $N = 3$ | $N = 4$ | $\overline{m}_b(\mu)$ | σ_N |
|-------|---------|---------------|---------|---------|-----------------------|------------|
| 5 | 4.0848 | 4.0799 | 4.0751 | 4.0707 | 4.0776 | 0.0053 |
| 10 | 3.6652 | 3.6509 | 3.6407 | 3.6551 | 3.6530 | 0.0088 |
| 15 | 3.4708 | 3.4457 | 3.4445 | 3.5290 | 3.4725 | 0.034 |

Table 2
 $m_b^{(N)}(\mu)$ as extracted from (6) via $S_N(\mu)$ truncated after three-loop terms. All entries are in GeV. The bold-face entry [$N = 2$, $\mu = 10$ GeV] corresponds to that preferred in Ref. [4] to generate $m_b(m_b)$.

One sees immediately from the table that this rms spread of values for $m_b(\mu)$ increases dramatically with μ , indicative of residual scale dependence. In other words, the error associated with different choices of N is itself a scale dependent quantity.

If Table 2 represents a valid determination of the quark mass, then for a fixed N , the variation of $m_b(\mu)$ with μ should conform with the RG evolution equation (11). However, the μ -dependence of $m_b(\mu)$ as extracted via Eq. (4) is not fully consistent with such evolution. In Figure 1, we have plotted the μ -dependence of such extracted values for the $N = 2$ case against the (three loop) RG-evolution following from Eq. (11) for values of μ between 5 GeV and 15 GeV. To facilitate this comparison, we evolve from the same value $m_b(10$ GeV) as extracted in Table 2 (in bold). The figure clearly shows a deviation by the μ -dependence extracted from Eq. (4) from that anticipated from RG-evolution. Moreover, this deviation becomes progressively pronounced with increased N . For $N = 4$, Figure 2 shows the plot of extracted versus RG-evolved μ dependence, which exhibits a substantially larger deviation for large μ , though a somewhat better fit between $\mu = 5$ GeV and $\mu = 10$ GeV.

These identifiable remaining scale dependences, both horizontal (N -dependence) and vertical (deviation from RG-evolution), necessarily percolate into estimates of $m_b(m_b)$. In Table 3 we display values of $m_b(m_b)$ obtained by evolving Eq. (4) values $m_b(\mu)$ extracted from Eq. (6) at the indicated scale μ . The values for $\mu = 10$ GeV, including the preferred $N = 2$ value, differ inconsequentially (they are 2 MeV larger) from the central values displayed in the erratum to Ref. [4], providing a check on our calculation. The column $\overline{m}_b(m_b)$ of Table 3 is just the average over N of $m_b(m_b)$ values, as evolved from the indicated choice of μ .

Similarly, the rms spread over N is just

$$\sigma_N = \frac{1}{2} \left[\sum_{N=1}^4 \left\{ m_b^{(N)}(m_b) - \overline{m}_b(m_b) \right\}^2 \right]^{1/2}, \quad (19)$$

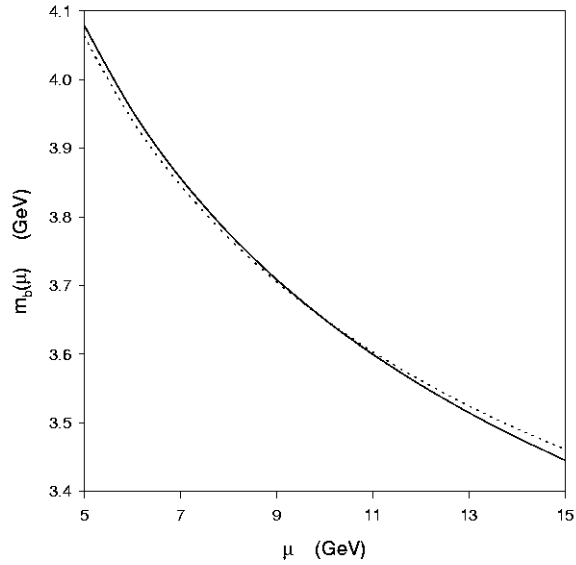


Fig. 1. Renormalization-scale (μ) dependence of $m_b(\mu)$ extracted via Eq. (6) (solid curve) for the $N = 2$ moment compared with the RG evolution of $m_b(\mu)$ (broken curve). For RG evolution, $m_b(10 \text{ GeV})$ is used as a reference scale, and hence the two curves intersect at $\mu = 10 \text{ GeV}$.

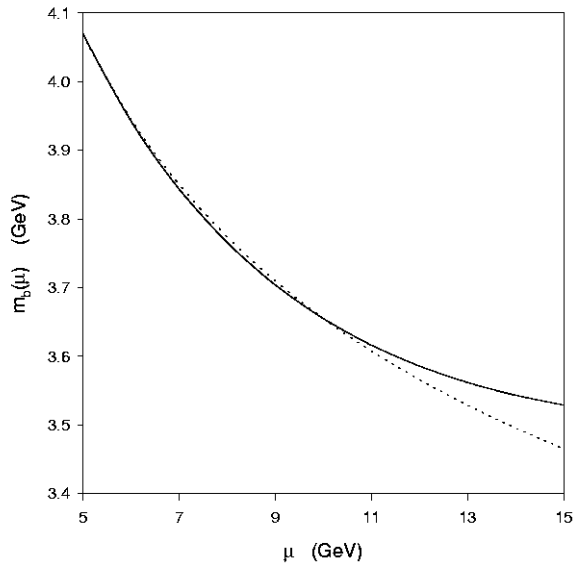


Fig. 2. Renormalization-scale (μ) dependence of $m_b(\mu)$ extracted via Eq. (6) (solid curve) for the $N = 4$ moment compared with the RG evolution of $m_b(\mu)$ (broken curve). For RG evolution, $m_b(10 \text{ GeV})$ is used as a reference scale, and hence the two curves intersect at $\mu = 10 \text{ GeV}$.

and the scale uncertainty (σ_μ) is just half the difference between the maximum and minimum value of $m_b(m_b)$ over a given column of the table. Thus σ_N is a measure of horizontal (N -dependence) uncertainty, and σ_μ is a measure of

| μ | $N = 1$ | $N = 2$ | $N = 3$ | $N = 4$ | $\overline{m}_b(m_b)$ | σ_N |
|--------------|---------|---------------|---------|---------|-----------------------|------------|
| 5 | 4.2116 | 4.2073 | 4.2031 | 4.1992 | 4.2053 | 0.0046 |
| 10 | 4.2067 | 4.1928 | 4.1830 | 4.1969 | 4.1948 | 0.0085 |
| 15 | 4.2025 | 4.1768 | 4.1755 | 4.2620 | 4.2042 | 0.035 |
| σ_μ | 0.005 | 0.015 | 0.014 | 0.033 | 0.0052 | |

Table 3
 $m_b^{(N)}(m_b)$ as RG-evolved from $m_b^{(N)}$ values listed in Table 2 (*i.e.*, via 3-loop-truncated series S_N). All entries are in GeV. The bold-faced entry [$N = 2, \mu = 10$] corresponds to preferred choices in Ref. [4].

vertical (μ -) renormalization-scale uncertainty. For the $N = 2$ $\mu = 10$ GeV preferred case [4], both of these uncertainties are indicative of overall 24 MeV theoretical uncertainties in $m_b(m_b)$ that devolve ultimately from residual scale dependence in truncating the series S_N .

3 Optimal RG-Improvement of the $\overline{\text{MS}}$ b -quark Mass

As noted in the previous section, the higher order $S_N(\mu)$ series coefficients $T_{1,1}^{(N)}$ and $T_{2,2}^{(N)}$ are determined via the RG-equation (8) from the leading series coefficient $T_{0,0}^{(N)}$. Similarly, the three-loop coefficient $T_{2,1}^{(N)}$ can be obtained via Eq. (17) from the one and two-loop series terms $T_{0,0}^{(N)}$ and $T_{1,0}^{(N)}$. In fact, the RG-equation (8) is much more powerful than any use we have made of it so far. Given the calculated values of $T_{0,0}^{(N)}$, $T_{1,0}^{(N)}$ and $T_{2,0}^{(N)}$, one can determine respectively *every* leading-logarithm (LL) coefficient $T_{j,j}^{(N)}$, *every* next-to-leading-logarithm (NLL) coefficient $T_{j,j-1}^{(N)}$, and *every* next-to-next-to-leading logarithm (NNLL) coefficient $T_{j,j-2}^{(N)}$ in the series expansion (7) for $S_N(\mu)$.

The procedure of optimal RG improvement [5] involves the summation to all orders of leading and progressively subleading logarithms within a series, a process that has been seen to reduce significantly the renormalization scale dependence in a wide variety of processes [5]. For the case at hand, we wish to include every RG-accessible coefficient $T_{j,k}^{(N)}$ in the series $S_N(\mu)$ in order to extract via Eq. (4) an $\overline{\text{MS}}$ b -quark mass $m_b(m_b)$ that is free (or nearly so) of the residual scale dependence evident in Table 3. To do this, we first organize the series (7) as follows:

$$S_N[x, L] = \sum_{n=0}^{\infty} x^n S_n^{(N)}(xL), \quad (20)$$

where

$$S_n^{(N)}(u) = \sum_{k=n}^{\infty} T_{k,k-n}^{(N)} u^{k-n} \quad (21)$$

with $u = xL$ amounts to an LL summation when $n = 0$, an NLL summation when $n = 1$, and an NNLL summation when $n = 2$. If we substitute Eq. (20) into Eq. (8), we generate a succession of first-order differential equations for these summations:

$$\left[(1 - \beta_0 u) \frac{d}{du} + 2N \right] S_0^{(N)}(u) = 0, \quad (22)$$

$$\left[(1 - \beta_0 u) \frac{d}{du} + (2N - \beta_0) \right] S_1^{(N)}(u) = \left[(\beta_1 u - 2) \frac{d}{du} - 2N\gamma_1 \right] S_0^{(N)}(u), \quad (23)$$

$$0 = - \left[(1 - \beta_0 u) \frac{d}{du} + (2N - 2\beta_0) \right] S_2^{(N)}(u) + \left[(\beta_1 u - 2) \frac{d}{du} + (\beta_1 - 2N\gamma_1) \right] S_1^{(N)}(u) + \left[(\beta_2 u - 2\gamma_1) \frac{d}{du} - 2N\gamma_2 \right] S_0^{(N)}(u). \quad (24)$$

Eq. (21) provides the initial conditions $S_0^{(N)}(0) = T_{0,0}^{(N)}$, $S_1^{(N)}(0) = T_{1,0}^{(N)}$, $S_2^{(N)}(0) = T_{2,0}^{(N)}$, the set of all known $T_{k,0}^{(N)}$ coefficients of the series $S_N(\mu)$ [see Table 1]. With these initial conditions, Eqs. (22)–(24) can be successively solved, and the optimally RG-improved series is found to be

$$S_N^{\Sigma}[xL] = S_0^{(N)}(xL) + xS_1^{(N)}(xL) + x^2S_2^{(N)}(xL). \quad (25)$$

For

$$w \equiv 1 - \beta_0 xL, \quad A \equiv -2N/\beta_0, \quad (26)$$

we find from Eqs. (22) and (23) that

$$S_0^{(N)}(xL) = T_{0,0}^{(N)} w^{-A}, \quad (27)$$

and

$$S_1^{(N)}(xL) = Bw^{-A} + [T_{1,0}^{(N)} - B + C \log w] w^{-A-1}, \quad (28)$$

with

$$B \equiv (\beta_1 A + 2N\gamma_1) T_{0,0}^{(N)} / \beta_0, \quad C \equiv (2\beta_0 - \beta_1) A T_{0,0}^{(N)} / \beta_0. \quad (29)$$

Substituting Eqs. (27) and (28) into Eq. (24) we obtain the solution

$$S_2^{(N)}(xL) = \frac{D}{2}w^{-A} + w^{-A-1} [E - F + F \log(w)] + w^{-A-2} \left[T_{2,0}^{(N)} - \frac{D}{2} - E + F + G \log(w) + \frac{H}{2} \log^2 w \right], \quad (30)$$

with

$$D = [\beta_1 AB + \beta_2 AT_{0,0}^{(N)} - (\beta_1 - 2N\gamma_1) B + 2N\gamma_2 T_{0,0}^{(N)}] / \beta_0, \quad (31)$$

$$E = \left[(2\beta_0 - \beta_1) AB + \beta_1 [(1+A)(T_{1,0}^{(N)} - B) - C] + (2\gamma_1\beta_0 - \beta_2) AT_{0,0}^{(N)} + (B - T_{1,0}^{(N)}) (\beta_1 - 2N\gamma_1) \right] / \beta_0, \quad (32)$$

$$F = C (A\beta_1 + 2N\gamma_1) / \beta_0, \quad (33)$$

$$G = [(1+A)(T_{1,0}^{(N)} - B) - C] (2\beta_0 - \beta_1) / \beta_0, \quad (34)$$

$$H = (2\beta_0 - \beta_1) (1+A)C / \beta_0. \quad (35)$$

The extraction of $m_b(m_b)$ now proceeds analogously to that in the previous section, except that the series $S_N(\mu)$ is now in the optimally RG-improved form (25), rather than the truncation

$$S_N = \sum_{j=0}^2 \sum_{k=0}^j T_{j,k}^{(N)} x^j L^k \quad (36)$$

of Eq. (7) to one-, two-, and three-loop contributions utilized in Section 2 (and employed in Ref. [4]). For a given choice of renormalization scale μ , the values of $m_b(\mu)$ we extract from Eqs. (4) and (25) are tabulated in Table 4. As before, the average $\overline{m_b}(\mu)$ is over $N = \{1, 2, 3, 4\}$ values of $m_b(\mu)$, and the rms spread over these values is given by Eq. (18). These spreads are seen to be significantly less than those of Table 2. We thus see that the extracted values for $m_b(\mu)$ from different values of N are in much better agreement when S_N is RG-improved. Moreover, the substantial increase of σ_N with μ characterizing Table 2 (and indicative of residual scale dependence) does *not* occur in Table 4. In Table 4, σ_N is essentially static at 4–5 MeV for μ between 5 and 15 GeV, corresponding to a small fixed theoretical uncertainty associated with the choice for N . Thus, RG-improvement is seen to disentangle (vertical) scale-uncertainties from (horizontal) N -uncertainties, as well as to reduce the magnitude of such N -uncertainties.

In contrast to Figs. 1 and 2, the Table 4 values of $m_b(\mu)$ extracted from Eq. (6) via the resummed S_N^Σ of Eq. (25) are fully consistent with the RG-evolution equation (11). For $N = 2$ Figure 3 plots both extracted values of $m_b(\mu)$ for

| μ | $N = 1$ | $N = 2$ | $N = 3$ | $N = 4$ | $\overline{m}_b(\mu)$ | σ_N |
|-------|---------|---------|---------|---------|-----------------------|------------|
| 5 | 4.0851 | 4.0797 | 4.0750 | 4.0717 | 4.0779 | 0.0050 |
| 10 | 3.6698 | 3.6653 | 3.6610 | 3.6582 | 3.6636 | 0.0044 |
| 15 | 3.4793 | 3.4751 | 3.4712 | 3.4687 | 3.4736 | 0.0040 |

Table 4

$m_b^{(N)}(\mu)$ as extracted from optimally RG-improved $S_N(\mu)$. All entries are in GeV. The average $m_b(\mu)$ and the rms spread σ_N over the four values of N are calculated as in Table 2. All entries are in GeV.

μ between 5 GeV and 15 GeV, as well as the values evolved [via Eq. (11)] directly from the extracted value $m_b^{(2)}(10 \text{ GeV}) = 3.6653 \text{ GeV}$. The points coincide to within the visual resolution of the figure, indicative of purely RG scale-dependence for values of $m_b(\mu)$ extracted via Eq. (25).⁵

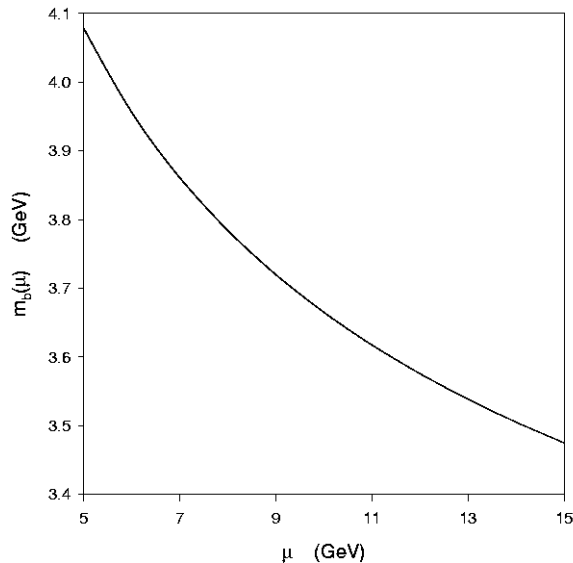


Fig. 3. Renormalization-scale (μ) dependence of $m_b(\mu)$ extracted via substitution of the resummed quantity S_N^Σ into (6) (solid curve) for the $N = 2$ moment compared with the RG evolution of $m_b(\mu)$ (broken curve). For RG evolution, $m_b(10 \text{ GeV})$ is used as a reference scale, and hence the two curves intersect at $\mu = 10 \text{ GeV}$. The two curves overlap completely within the resolution of the figure. Similar overlap occurs for all other moments considered (*i.e.* $N = 1, 3, 4$).

The absence of any additional residual scale dependence naturally carries over to the RG-evolution of extracted $m_b(\mu)$ to $m_b(m_b)$. In Table 5 we list values of $m_b(m_b)$ obtained by evolution of the value $m_b(\mu)$ extracted at the scale μ for the indicated moments N . RG-improvement is seen in Table 4 to virtually

⁵ The difference between extracted and evolved values at $\mu = 15 \text{ GeV}$ is less than 10^{-4} GeV , based on identical starting values at $\mu = 10 \text{ GeV}$.

| μ | $N = 1$ | $N = 2$ | $N = 3$ | $N = 4$ | $\overline{m_b}(m_b)$ | σ_N |
|--------------|---------|---------|---------|---------|-----------------------|------------|
| 5 | 4.2118 | 4.2071 | 4.2030 | 4.2002 | 4.2055 | 0.0044 |
| 10 | 4.2112 | 4.2068 | 4.2027 | 4.2002 | 4.2052 | 0.0042 |
| 15 | 4.2111 | 4.2069 | 4.2028 | 4.2003 | 4.2053 | 0.0041 |
| σ_μ | 0.0007 | 0.0003 | 0.0003 | 0.0001 | 0.0003 | |

Table 5
 $m_b^{(N)}(m_b)$ as RG-evolved from $m_b^{(N)}(\mu)$ values listed in Table 4 (*i.e.*, via the RG-improved series S_N^Σ). $\overline{m_b}(m_b)$, the average of $m_b(m_b)$ over N , σ_N , the rms spread over N , and the scale uncertainty σ_μ are obtained as in Table 2. All entries are in GeV.

eliminate the scale uncertainty (σ_μ) evident in Table 3. The only theoretical uncertainty still evident is horizontal, the σ_N associated with different choices of N , and this uncertainty is both small ($\mathcal{O}(4 \text{ MeV})$) and static as μ varies from 5 to 15 GeV. For Ref. [4]’s phenomenologically motivated choice $\mu = 10 \text{ GeV}$, σ_N for the RG improved case (Table 5) is less than half the value for σ_N when S_N is truncated (Table 3).

This virtual elimination of residual scale dependence, as evident in Table 5, also leads to a changed central value for $m_b(m_b)$ relative to that of the erratum to Ref. [4]. The central value quoted in the erratum is 4.191 GeV, based on choices $\mu = 10 \text{ GeV}$, $N = 2$. The corresponding value in our Table 3 is 4.193 GeV, and the 2 MeV discrepancy is insignificant compared to the erratum estimate of theoretical uncertainty ($\pm 51 \text{ MeV}$), or relative to Table 3’s $\pm 15 \text{ MeV}$ and $\pm 9 \text{ MeV}$ vertical and horizontal theoretical uncertainties associated with the choice of μ and N . The corresponding $N = 2$, $\mu = 10 \text{ GeV}$ value in Table 5 is 4.207 GeV with aggregate 4.5 MeV horizontal and vertical uncertainties.

Thus, the incorporation of an optimally RG-improved perturbative series $S_N(\mu)$ is seen to eliminate the renormalization-scale theoretical uncertainty and halve the moment-dependence theoretical uncertainty, with a 14 MeV increase in the corresponding central value 4.207 GeV. Note the near equivalence of this value with the $m_b(m_b) = 4.205 \text{ GeV}$ values found from the $\overline{m_b}(m_b)$ averages over the first four moments (Table 5).

4 Residual Scale Dependence of the Pole Mass

The series $T(\mu) = T[x(\mu), L(\mu)]$ relating the (RG-invariant) pole b -quark mass M_b^p and the $\overline{\text{MS}}$ mass $m_b(\mu)$ is given by

$$M_b^p = m_b(\mu)T[x(\mu), L(\mu)], \quad (37)$$

$$T[x, L] = 1 + \sum_{j=0}^{\infty} \sum_{k=0}^j T_{j,k} x^j L^k, \quad (38)$$

where $x(\mu) = \alpha_s(\mu)/\pi$ and $L(\mu) = \log(\mu^2/m_b^2(\mu))$ as before, and where the known series coefficients in the $L = 0$ limit are [6]

$$\begin{aligned} T_{1,0} &= 4/3, \\ T_{2,0} &= -1.0414(n_f - 1) + 13.4434 \xrightarrow{n_f=5} 9.2778 \\ T_{3,0} &= 0.6527(n_f - 1)^2 - 26.655(n_f - 1) + 190.595 \xrightarrow{n_f=5} 94.4182 \end{aligned} \quad (39)$$

If one wishes to relate the pole mass to $m_b(m_b)$ (*i.e.*, to the point $\mu = m_b(\mu)$), all logarithms in the series (38) are zero and only the coefficients $T_{j,0}$ contribute.

Since M_b^p is a RG-invariant quantity, renormalization scale dependence can be studied by explicitly varying $m_b(\mu)$ through the RG equation as μ is varied. Given the residual scale dependence implicit in any truncation of the series (38), one can argue that the choice of scale μ , generally motivated by experimental information [as is used to determine M_N^{exp} via Eq. (3)], should be consistently maintained. For example, the benchmark mass $m_b(m_b)$ is obtained in Ref. [4] via a determination of $m_b(10 \text{ GeV})$, and then by subsequent evolution [Eq. (11)] to the point $\mu = m_b(\mu)$.

A measure of the residual scale-dependence implicit in the determination of the pole mass from the $\overline{\text{MS}}$ mass obtained via Ref. [4] methodology would be the difference between

- (1) the $\mu = 10 \text{ GeV}$ pole mass obtained via Eqs. (37) and (38) by incorporating within the logarithm $L(\mu)$ the value $m_b(10 \text{ GeV})$ actually extracted from Eq. (6), and
- (2) the $\mu = m_b(m_b)$ pole mass obtained via Eqs. (37) and (38) from similar incorporation of $m_b(m_b)$, as evolved via Eq. (11) from the extracted value $m_b(10 \text{ GeV})$.

We emphasize that if the input values $m_b(m_b)$ and $m_b(10 \text{ GeV})$ are RG-consistent, then any discrepancy between M_b^p obtained by these two proce-

dures is a reflection of residual scale dependence arising solely from the truncation of the series (38).

To implement this comparison, we need to know the coefficients $T_{j,k}$ with $k \neq 0$ for $j = \{1, 2, 3\}$. Since the pole mass is an RG-invariant, $dM_b^p/d\mu^2 = 0$. One then finds from Eq. (37) the following RG-equation for the series $T[x, L]$:

$$\left[(1 - 2\gamma(x)) \frac{\partial}{\partial L} + \beta(x) \frac{\partial}{\partial x} + \gamma(x) \right] T[x, L] = 0 \quad (40)$$

If one substitutes the series (38) into the above equation, and then utilizes the series (11) and (13) for $\gamma(x)$ and $\beta(x)$, one finds after a little algebra that

$$T_{1,1} = 1, \quad T_{2,2} = (1 + \beta_0) / 2 \xrightarrow{n_f=5} \frac{35}{24}, \quad (41)$$

$$T_{2,1} = (1 + \beta_0) T_{1,0} + \gamma_1 - 2 \xrightarrow{n_f=5} 5.4208 \quad (42)$$

$$T_{3,3} = (1 + \beta_0) (1 + 2\beta_0) / 6 \xrightarrow{n_f=5} \frac{1015}{432}, \quad (43)$$

$$T_{3,2} = (1 + \beta_0) (1 + 2\beta_0) T_{1,0} / 2 + \beta_0 (\gamma_1 - 3) + \gamma_1 + \frac{\beta_1}{2} - 2 \xrightarrow{n_f=5} 13.1053, \quad (44)$$

$$T_{3,1} = (1 + 2\beta_0) T_{2,0} + (\beta_1 + \gamma_1 - 2\beta_0 - 2) T_{1,0} + \gamma_2 - 4\gamma_1 + 4 \xrightarrow{n_f=5} 42.3366 \quad (45)$$

We then can employ the three-loop series

$$T[x, L] = \sum_{j=1}^3 \sum_{k=0}^j T_{j,k} x^j L^k \quad (46)$$

with series coefficients given in Eqs. (39) and (41)–(45) to compare the pole mass obtained from the extracted value $m_b(10 \text{ GeV})$ to that from the correspondingly RG-evolved value $m_b(m_b)$. To be consistent with having three subleading orders in x in series (38), we utilize Eqs. (11) and (13) to four-loop order to evolve $x(\mu)$ and $m_b(\mu)$ [$\beta_3 = 18.8522$ [11], $\gamma_3 = 11.0343$ [13]] from the same $x(10 \text{ GeV}) = 0.056732$ reference couplant value [as evolved from an assumed $\alpha_s(M_Z) = 0.11800$] used throughout. Using the $\mu = 10 \text{ GeV}$, $N = 2$ value $m_b^{(2)}(10 \text{ GeV}) = 3.651 \text{ GeV}$ of Table 2 as a springboard value, and its corresponding value $m_b(m_b) = 4.19 \text{ GeV}$ (Table 3), we find somewhat different pole masses for different choices of μ :

$$\mu = 10 \text{ GeV}, \quad M_b^p = 4.82 \text{ GeV}, \quad (47)$$

$$\mu = 4.19 \text{ GeV}, \quad M_b^p = 4.94 \text{ GeV}, \quad (48)$$

indicative of 120 MeV residual scale uncertainty. We emphasize that this uncertainty arises entirely from the truncation of the series (38), and is independent of scale uncertainties in the extraction of $m_b(\mu)$. Had we used the corresponding $N = 2$, $\mu = 10$ GeV values $m_b(10 \text{ GeV}) = 3.665 \text{ GeV}$, $m_b(m_b) = 4.21 \text{ GeV}$ obtained in Tables 4 and 5 via optimal RG improvement, the corresponding pole masses still exhibit virtually the same residual scale uncertainty:

$$\mu = 10 \text{ GeV}, \quad M_b^p = 4.84 \text{ GeV}, \quad (49)$$

$$\mu = 4.21 \text{ GeV}, \quad M_b^p = 4.95 \text{ GeV}. \quad (50)$$

Consequently, there appears to be a surprisingly large 110–120 MeV theoretical uncertainty implicit in the determination of the pole mass from the $\overline{\text{MS}}$ mass $m_b(\mu)$, an uncertainty devolving ultimately from truncation of the series (38) after its $\mathcal{O}(x^3)$ terms. In the section which follows, we will optimally RG-improve the series (38) to reduce this residual scale uncertainty by a factor of 15.

5 Optimal RG Improvement of the Pole Mass

Optimal RG-improvement of the series $T[x, L]$ follows along the same lines as described in Section 3 for the series $S_N[x, L]$. We express the series (38) in the form

$$T[x, L] = \sum_{n=0}^{\infty} T_n(xL)x^n \quad (51)$$

where

$$T_n(u) = \sum_{k=n}^{\infty} T_{k,k-n} u^{k-n} \quad (52)$$

with $T_0(xL)$ encompassing the LL summation (all values of $T_{k,k}$), $T_1(xL)$ encompassing the NLL summation, *etc.* Since $T_{3,0}$ is known [Eq. (39)], the functions $T_0(xL)$, $T_1(xL)$, $T_2(xL)$ and the N³LL summation $T_3(xL)$ within Eq. (51) are all RG accessible. If we substitute Eq. (51) into the RG-equation (40), we find the following set of sequentially solvable first order differential equations for $T_n(u)$, $n = \{0, 1, 2, 3\}$, with initial conditions $T_n(0) = T_{n,0}$ [Eq. (52)] explicitly listed in Eq. (39):

$$\left[(1 - \beta_0 u) \frac{d}{du} - 1 \right] T_0(u) = 0, \quad (53)$$

$$\left[(1 - \beta_0 u) \frac{d}{du} - (1 + \beta_0) \right] T_1(u) = \left[(\beta_1 u - 2) \frac{d}{du} + \gamma_1 \right] T_0(u), \quad (54)$$

$$0 = - \left[(1 - \beta_0 u) \frac{d}{du} - (1 + 2\beta_0) \right] T_2(u) + \left[(\beta_1 u - 2) \frac{d}{du} + (\gamma_1 + \beta_1) \right] T_1(u) \\ + \left[(\beta_2 u - 2\gamma_1) \frac{d}{du} + \gamma_2 \right] T_0(u), \quad (55)$$

$$0 = - \left[(1 - \beta_0 u) \frac{d}{du} - (1 + 3\beta_0) \right] T_3(u) + \left[(\beta_1 u - 2) \frac{d}{du} + (\gamma_1 + 2\beta_1) \right] T_2(u) \\ + \left[(\beta_2 u - 2\gamma_1) \frac{d}{du} + (\gamma_2 + \beta_2) \right] T_1(u) + \left[(\beta_3 u - 2\gamma_2) \frac{d}{du} + \gamma_3 \right] T_0(u). \quad (56)$$

Given $u = xL$ and the definition $w \equiv 1 - \beta_0 xL$, the solutions to the above four equations are

$$T_0(xL) = w^{-A}, \quad (57)$$

$$T_1(xL) = Bw^{-A} + w^{-A-1} [T_{1,0} - B + C \log(w)], \quad (58)$$

$$T_2(xL) = \frac{D}{2} w^{-A} + w^{-A-1} [E - F + F \log(w)] \\ + w^{-A-2} \left[T_{2,0} - \frac{D}{2} - E + F + G \log(w) + \frac{H}{2} \log^2(w) \right], \quad (59)$$

$$T_3(xL) = \frac{K}{3} w^{-A} + w^{-A-1} \left(\frac{M}{2} - \frac{N}{4} + \frac{N}{2} \log(w) \right) \\ + w^{-A-2} [P - Q + 2R + (Q - 2R) \log(w) + R \log^2(w)] \\ + w^{-A-3} \left\{ -\frac{K}{3} - \frac{M}{2} + \frac{N}{4} - P + Q - 2R + T_{3,0} + U \log(w) \right. \\ \left. + \frac{V}{2} \log^2(w) + \frac{Y}{3} \log^3(w) \right\}, \quad (60)$$

where parameters $A - Y$ are now given by

$$A = 1/\beta_0, \quad B = (A\beta_1 - \gamma_1)/\beta_0, \quad C = (2\beta_0 - \beta_1) A/\beta_0, \quad (61)$$

$$D = [\beta_1 AB + \beta_2 A - (\beta_1 + \gamma_1) B - \gamma_2]/\beta_0, \quad (62)$$

$$\beta_0 E = (2\beta_0 - \beta_1) AB + [(1 + A)(T_{1,0} - B) - C] \beta_1 \\ + (2\beta_0 \gamma_1 - \beta_2) A + (B - T_{1,0})(\beta_1 + \gamma_1), \quad (63)$$

$$F = (A\beta_1 - \gamma_1) C/\beta_0, \quad (64)$$

$$G = [(1 + A)(T_{1,0} - B) - C] (2\beta_0 - \beta_1)/\beta_0, \quad (65)$$

$$H = (2\beta_0 - \beta_1) (1 + A) C/\beta_0, \quad (66)$$

$$\beta_0 K = [A(\beta_3 + \beta_2 B + \beta_1 D/2) - B(\gamma_2 + \beta_2) - \gamma_3 + (\gamma_1 + 2\beta_1) D/2], \quad (67)$$

$$\beta_0 M = [(2\beta_0 \gamma_2 - \beta_3) + B(2\beta_0 \gamma_1 - \beta_2) + D(2\beta_0 - \beta_1)/2] A \\ + [\gamma_2 + \beta_2 - (A + 1)\beta_2] (B - T_{1,0}) - C\beta_2 \\ + (\gamma_1 + 2\beta_1) (F - E) + [E(1 + A) - F(2 + A)] \beta_1, \quad (68)$$

$$N = [C(A\beta_2 - \gamma_2) + F[(A-1)\beta_1 - \gamma_1]]/\beta_0, \quad (69)$$

$$\begin{aligned} \beta_0 P &= (2\beta_0\gamma_1 - \beta_2)[(1+A)(T_{1,0} - B) - C] \\ &\quad + (2\beta_0 - \beta_1)[(1+A)E - (2+A)F] \\ &\quad - (\gamma_1 + 2\beta_1)(T_{2,0} - D/2 - E + F) \\ &\quad - \beta_1[G - (2+A)](T_{2,0} - D/2 - E + F), \end{aligned} \quad (70)$$

$$\begin{aligned} \beta_0 Q &= [(2\beta_0\gamma_1 - \beta_2)C + (2\beta_0 - \beta_1)F](1+A) \\ &\quad - (\gamma_1 + 2\beta_1)G - [H - (2+A)G]\beta_1, \end{aligned} \quad (71)$$

$$R = (\beta_1 A - \gamma_1)H/2\beta_0, \quad (72)$$

$$U = (2\beta_0 - \beta_1)[(2+A)(T_{2,0} - D/2 - E + F) - G]/\beta_0, \quad (73)$$

$$V = (2\beta_0 - \beta_1)[(2+A)G - H]/\beta_0, \quad (74)$$

$$Y = (2\beta_0 - \beta_1)(2+A)H/2\beta_0. \quad (75)$$

We now can compare the pole mass obtained via Eq. (37) from the first four terms of the series (51), which include all RG-accessible coefficients,

$$T[x, L] = T_0(xL) + xT_1(xL) + x^2T_2(xL) + x^3T_3(xL), \quad (76)$$

to the pole mass obtained via the three-loop series (46). If we utilize Table 5's $N = 2$, $\mu = 10$ GeV extracted value $m_b(10 \text{ GeV}) = 3.665$ GeV and incorporate Eq. (76) into Eq. (37), we find that

$$\mu = 10 \text{ GeV}, \quad M_b^p = 4.959 \text{ GeV} \quad (77)$$

$$\mu = 4.207 \text{ GeV}, \quad M_b^p = 4.951 \text{ GeV} \quad (78)$$

This $\mathcal{O}(8 \text{ MeV})$ uncertainty is a remarkable improvement over the $\mathcal{O}(110 \text{ MeV})$ uncertainty [Eqs. (49) and (50)] following from the same input assumptions, but with $T[x, L]$ given by the three loop series (46). Thus, the RG-improved series (76) removes virtually all the residual scale dependence in the relation between the pole and $\overline{\text{MS}}$ mass. This is corroborated in Fig. 4, in which the pole masses obtained via the three loop series (46) and the RG-improved series (76) are compared directly, given identical $m_b(10 \text{ GeV}) = 3.6636$ GeV anchoring values for the $\overline{\text{MS}}$ mass [the $\mu = 10$ GeV value for $\overline{m}_b(m_b)$ in Table 4]. The pole mass for the RG-improved case exhibits very little dependence on μ . Thus optimal RG-improvement of the perturbative series (38) is seen to remove virtually all of the substantial ($\mathcal{O}(110\text{--}120 \text{ MeV})$) residual uncertainty characterizing the relationship between the $\overline{\text{MS}}$ and the pole b -quark mass.

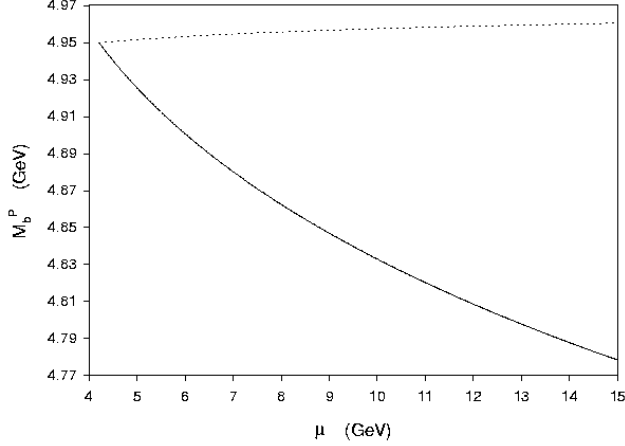


Fig. 4. Renormalization scale dependence of the resummed expression of the pole mass (broken curve) compared with the unsummed expression (solid curve). The $\overline{\text{MS}}$ mass $m_b(\mu)$ used as input to this comparison is based on RG evolution from the reference value $m_b(10 \text{ GeV}) = 3.66 \text{ GeV}$ as outlined in the text.

6 Optimal RG Improvement of M_b^{1S}/M_b^p

The b -quark $1S$ mass (M_b^{1S}), defined to be half the perturbative mass of a (theoretical) $3S_1$ $b\bar{b}$ meson, has been determined via relations between masses and widths of Υ mesons to moments of the b -quark vector current correlation function [14]. This $1S$ mass is related to the pole mass M_b^p (which is much more sensitive to Λ_{QCD}) via the perturbative relationship [7,8],

$$M_b^{1S} = M_b^p \left[1 - \frac{2\pi^2 x^2(\mu)}{9} W(\mu) \right], \quad (79)$$

for which the series $W(\mu)$ is known in full to two subleading orders:

$$W(\mu) = W[x(\mu), \ell(\mu)] \quad , \quad \ell(\mu) = \log \left[\frac{3\mu}{4\pi x(\mu) M_b^p} \right], \quad (80)$$

$$W[x, \ell] = 1 + \sum_{n=1}^{\infty} \sum_{m=0}^n \tau_{n,m} x^n \ell^m \quad (81)$$

where

$$\tau_{1,0} = \frac{97}{6} - \frac{11n_f}{9} \xrightarrow{n_f=5} \frac{181}{18} \quad (82)$$

$$\tau_{2,0} = 337.95 - 40.965n_f + 1.1629n_f^2 \xrightarrow{n_f=5} 162.19 \quad (83)$$

$$\tau_{1,1} = 4\beta_0 \xrightarrow{n_f=5} \frac{23}{3} \quad (84)$$

$$\tau_{2,1} = 6\beta_0\tau_{1,0} - 8\beta_0^2 + 4\beta_1 \xrightarrow{n_f=5} \frac{1151}{12} \quad (85)$$

$$\tau_{2,2} = 12\beta_0^2 \xrightarrow{n_f=5} \frac{529}{12}. \quad (86)$$

In principle, M_b^{1S} and M_b^p are both RG-invariant entities independent of the renormalization scale μ . Consequently, one can obtain the following RG-equation for $W[x, \ell]$ by requiring that $\frac{d}{d\mu^2} [x^2(\mu)W(\mu)] = 0$:

$$\left[2\beta(x) + x\beta(x)\frac{\partial}{\partial x} + \left[\frac{x}{2} - \beta(x) \right] \frac{\partial}{\partial \ell} \right] W[x, \ell] = 0, \quad (87)$$

with $\beta(x)$ given by Eq. (13). If one substitutes the series (81) into the RG-equation (87), one easily corroborates the results (84)–(86).

Optimal RG improvement of the series $W[x, \ell]$ is obtained by expressing the series in the form

$$W[x, \ell] = \sum_{n=0}^{\infty} x^n W_n(x\ell) \quad (88)$$

where

$$W_n(x\ell) = \sum_{k=n}^{\infty} \tau_{k,k-n}(x\ell)^{k-n}. \quad (89)$$

As before, the series $W_0(x\ell)$ is inclusive of all LL coefficients $\tau_{k,k}$ in the series (81). Similarly, $W_1(x\ell)$ includes all NLL coefficients $\tau_{k,k-1}$, and $W_2(x\ell)$ includes all NNLL coefficients $\tau_{k,k-2}$. Upon substituting Eq. (88) into the RG equation (87), we obtain successive first order differential equations for the $n = \{0, 1, 2\}$ cases of series (89):

$$\left[(1 - 2\beta_0 u) \frac{d}{du} - 4\beta_0 \right] W_0(u) = 0, \quad (90)$$

$$\left[(1 - 2\beta_0 u) \frac{d}{du} - 6\beta_0 \right] W_1(u) = \left[2(\beta_1 u - \beta_0) \frac{d}{du} + 4\beta_1 \right] W_0(u), \quad (91)$$

$$\begin{aligned} \left[(1 - 2\beta_0) \frac{d}{du} - 8\beta_0 \right] W_2(u) &= [2(\beta_1 u - \beta_0) + 6\beta_1] W_1(u) \\ &+ [2(\beta_2 u - \beta_1) + 4\beta_2] W_0(u). \end{aligned} \quad (92)$$

Given the initial conditions $W_0(0) = \tau_{0,0} = 1$, $W_1(0) = \tau_{1,0}$ and $W_2(0) = \tau_{2,0}$ evident from the definition (89) of $W_n(u)$, we obtain the following solutions to Eqs. (90), (91) and (92):

$$W_0(x\ell) = (1 - 2\beta_0 x\ell)^{-2} \quad (93)$$

$$W_1(x\ell) = (1 - 2\beta_0 x\ell)^{-3} \left[\tau_{1,0} + 4 \left(\beta_0 - \frac{\beta_1}{2\beta_0} \right) \log(1 - 2\beta_0 x\ell) \right], \quad (94)$$

$$W_2(x\ell) = \mathcal{U}(1 - 2\beta_0 x\ell)^{-3} + \frac{[\tau_{2,0} - \mathcal{U} + \mathcal{V}\mathcal{X} \log(1 - 2\beta_0 x\ell) + 3\mathcal{V}^2 \log^2(1 - 2\beta_0 x\ell)]}{(1 + 2\beta_0 x\ell)^4}, \quad (95)$$

where

$$\mathcal{U} = 2 \left[\frac{\beta_1^2}{\beta_0^2} - \frac{\beta_2}{\beta_0} \right], \quad (96)$$

$$\mathcal{V} = (\beta_1 - 2\beta_0^2) / \beta_0, \quad (97)$$

$$\mathcal{X} = -3\tau_{1,0} + 4\beta_0 - 2\beta_1/\beta_0, \quad (98)$$

with $\tau_{1,0}$ and $\tau_{2,0}$ as given in Eq. (86).

Let us first consider any residual scale dependence in the relation (79) arising from truncation of the series (81) after the known coefficients (86). It has been argued in Ref. [9] that the relation (79) is to be utilized at soft momentum scales ($1.5 \text{ GeV} < \mu < 3.5 \text{ GeV}$), because the $1S$ mass is defined purely from nonrelativistic dynamics. Moreover, a soft scale necessarily follows from the non-perturbative nature of the logarithm ℓ ; if μ is hard, then x is small and logarithms are large. Given Eq. (77)'s b -quark pole mass of 4.96 GeV, for example, we find for the truncated series that the $1S$ b -quark mass varies between 4.58 and 4.73 GeV as μ increases from 1.5 and 3.5 GeV, a 150 MeV residual scale uncertainty. This range is substantially diminished if we utilize the RG-improved series

$$W[x, \ell] = W_0(x\ell) + xW_1(x\ell) + x^2W_2(x\ell), \quad (99)$$

as determined by Eqs. (93), (94) and (95), for the same region of μ . For the RG improved series, we find that the $1S$ b -quark mass corresponding to a 4.96 GeV pole mass varies between 4.66 GeV and 4.61 GeV as μ increases from 1.5 GeV to 3.5 GeV. Thus, optimal RG improvement reduces the residual scale uncertainty from 150 MeV to 50 MeV. These results are presented graphically in Fig. 5.

It is, of course, more realistic to extract a b -quark pole mass from a phenomenological determination of the $1S$ b -quark mass. Using the central value 4.71 GeV for the $1S$ mass [9], one can invert the relation (79) numerically for both the truncated and the RG-improved versions of the series (81). The results of this inversion are displayed in Fig. 6, and are indicative of a pole mass somewhat above 5 GeV. Once again, however, an $\mathcal{O}(150 \text{ MeV})$ theoretical scale uncertainty for the truncated case is reduced to a 40 MeV scale uncertainty using the RG improved series. Note that the crossing point in both figures is the soft- μ point at which the logarithm ℓ is equal to zero. It is evident from the initial conditions for W_0 , W_1 and W_2 that the RG summed series and the truncated series are equivalent at this point.

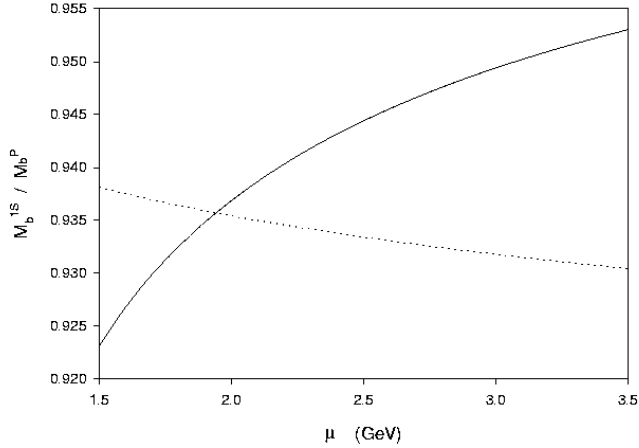


Fig. 5. Renormalization scale dependence of the resummed expression of the ratio M_b^{1S}/M_b^P (broken curve) compared with the unsummed expression (solid curve). The range considered for μ is the “soft” region advocated in [9], and $M_b^P = 4.96$ GeV is used as an input value.

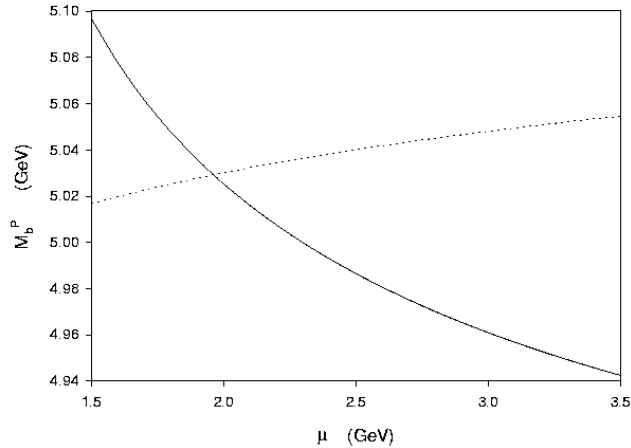


Fig. 6. Renormalization scale dependence of the resummed expression for M_b^P (broken curve) compared with the unsummed expression (solid curve). The input value $M_b^{1S} = 4.71$ GeV and the range considered for μ follows from Ref. [9].

7 Conclusions

The procedure for extracting the $\overline{\text{MS}}$ mass from empirical moments M_N of $R(s)$ necessarily exhibits dependence on both the choice of renormalization scale (μ) and the choice of moment (N), as demonstrated in Section 2. Omitting coupling-constant and experimental uncertainties, we have shown that an analysis based upon the Ref. [4] choices $\mu = 10$ GeV and $N = 2$ leads to the

extraction of an $\overline{\text{MS}}$ b -quark mass

$$m_b(m_b) = 4.193 \text{ GeV} \pm 15 \text{ MeV} \pm 8.5 \text{ MeV}. \quad (100)$$

The first theoretical uncertainty is associated with a ± 5 GeV variation of the renormalization scale μ , and the second reflects the moment dependence in letting the choice of moment N vary from 1 to 4.

In Section 3, the perturbative series (7) from which this prediction is obtained is optimally RG-improved via the all-orders summation of that series' leading, next-to-leading, and next-to-next-to-leading logarithms, *i.e.*, the summation of all RG-accessible logarithms in the perturbative series. If input assumptions leading to Eq. (100) are otherwise unchanged, the optimally RG-improved $\overline{\text{MS}}$ mass is then found to be

$$m_b(m_b) = 4.207 \text{ GeV} \pm 0.3 \text{ MeV} \pm 4.2 \text{ MeV}. \quad (101)$$

As before, the renormalization-scale and moment-dependence uncertainties displayed above are associated respectively with varying μ by ± 5 GeV and varying N from 1 to 4.

The reduction in this latter uncertainty associated with the choice of moment N is an unanticipated but welcome feature of the RG-improvement developed in Section 3. Indeed, prior to such improvement the uncertainty (σ_N) devolving from varying N is seen in Table 3 to increase quite drastically with μ ($\sigma_N = 35$ MeV at $\mu = 15$ GeV). After RG-improvement, however, this N -uncertainty is reduced to 4 MeV levels regardless of the choice for μ (Table 5).

Renormalization scale dependence inherent in relations between the b -quark pole mass and corresponding b -quark $\overline{\text{MS}}$ and $1S$ masses is shown in Sections 5 and 6 to be similarly reduced via optimal RG-improvement of the perturbative series characterizing such relations. Comparison of “RG-unimproved” extractions of the pole mass [Eqs. (49) and (50)] to RG-improved extractions [Eqs. (77) and (78)] for which all input information is otherwise equivalent indicates a reduction from 110 MeV to 8 MeV in the variation of the pole mass with renormalization scale as that scale varies from 4.2 GeV to 10 GeV. Moreover, for the improved case, the central-value pole mass is found to be near the high end of the range for the “unimproved” pole mass. A similar elevation with RG-improvement characterizes the pole mass extracted from the $1S$ mass, as discussed in Section 6. In Fig. 6, the summation of RG-accessible logarithms is shown to lead to a less scale-dependent and somewhat larger pole mass extracted from an assumed 4.71 GeV b -quark $1S$ -mass than would occur in the absence of such RG-improvement. In particular, there is a reduction from 140 MeV to 40 MeV in the variation of the pole mass as the renormalization scale μ varies between 1.5 GeV and 3.5 GeV.

The important point common to all of the cases considered above, however, is that (often-ignored) theoretical uncertainties necessarily follow from the residual renormalization-scale dependence characterizing the truncation of phenomenological perturbative series, and that such uncertainties may be substantially reduced, if not eliminated, by improving such series to include summation of all higher order RG-accessible contributions. Such resummation techniques should thus prove to be of increasing value as phenomenological and experimental inputs into b -mass determinations become more precise.

8 Acknowledgments

Research funding from the Natural Science and Engineering Research Council of Canada (NSERC) is gratefully acknowledged. Ailin Zhang is partly supported by National Natural Science Foundation of China.

References

- [1] V.A. Novikov, L.B. Okun, M.A. Shifman, A.I. Vainshtein, M.B. Voloshin and V.I. Zakharov, Phys. Rep. C 41 (1978) 1.
- [2] J.Z. Bai, *et. al.* (BES collaboration) Phys. Rev. Lett. 88 (2002) 101802.
- [3] K.G. Chetyrkin, J.H. Kühn, M. Steinhauser, Phys. Lett. B 371 (1996) 93; Nucl. Phys. B 482 (1996) 213; Nucl. Phys. B 505 (1997) 40.
- [4] J.H. Kühn, M. Steinhauser, Nucl. Phys. B 619 (2001) 588; Erratum Nucl. Phys. B 640 (2002) 415.
- [5] M.R. Ahmady, F.A. Chishtie, V. Elias, A.H. Fariborz, N. Fattahi, D.G.C. McKeon, T.N. Sherry, T.G. Steele, Phys.Rev. D66 (2002) 014010; M.R. Ahmady, F.A. Chishtie, V. Elias, A.H. Fariborz, D.G.C. McKeon, T.N. Sherry, A. Squires, T.G. Steele, Phys.Rev. D67 (2003) 034017.
- [6] N. Gray, D.J. Broadhurst, W. Grafe and K. Schilcher, Z. Phys. C 48 (1990) 673; D.J. Broadhurst, N. Gray and K. Schilcher, Z. Phys. C 52 (1991) 111; J. Fleischer, F. Jegerlehner, O.V. Tarasov and O.L. Veretin, Nucl. Phys. B 539 (1999) 671; K.G. Chetyrkin, M. Steinhauser Phys. Rev. Lett. 83 (1999) 4001; K. Melnikov, T. van Ritbergen, Phys. Lett. B482 (2000) 99; K.G. Chetyrkin and M. Steinhauser, Nucl. Phys. B 573 (2000) 617.
- [7] A. Pineda, F.J. Yndurain, Phys. Rev. D58 (1998) 094022; K. Melnikov, A. Yelkhovsky, Phys. Rev. D59 (1999) 114009.

- [8] A.H. Hoang, T. Teubner, Phys. Rev. D60 (1999) 114027.
- [9] A.H. Hoang, Phys. Rev. D61 (2000) 034005.
- [10] D.J. Gross and F. Wilczek, Phys. Rev. Lett. 30 (1973) 1343; H.D. Politzer, Phys. Rev. Lett. 30 (1973) 1346;
W.E. Caswell, Phys. Rev. Lett. 33 (1974) 244;
D.R.T. Jones, Nucl. Phys. B 75 (1974) 531;
E.S. Egorian, O.V. Tarasov, Theor. Mat. Fiz. 41 (1979) 26;
O.V. Tarasov, A.A. Vladimirov, and A. Yu. Zharkov, Phys. Lett. B 93 (1980) 429;
S.A. Larin and J.A.M. Vermaseren, Phys. Lett. B 303 (1993) 334.
- [11] T. van Ritbergen, J.A.M. Vermaseren, S.A. Larin, Phys. Lett. B400 (1997) 379.
- [12] R. Tarrach, Nucl. Phys. B183 (1981) 384.
- [13] K.G. Chetyrkin, Phys. Lett. B404 (1997) 161.
- [14] A.H. Hoang, Z. Ligeti, A.V. Manohar, Phys. Rev. Lett. 82 (1999) 277 and Phys. Rev. D59 (1999) 074017.